

NMR Determination of Keto–Enol Equilibrium Constants

Dustin Wheeler

Thursday 4th March, 2021

In this experiment, the barrier to rotation in *N,N*-dimethylacetamide can be determined by measuring changes in ¹H-NMR line shapes as a function of temperature. This study is an example of dynamic NMR spectroscopy (spectroscopy on a changing system, as opposed to a static one).¹

¹ Transcribed from Gasparro and Kolodny [1] and Nibler et al. [2].

Theory

Magnetic Moments

The magnetic moment of a nucleus with nuclear spin quantum number I is

$$\mu = g_N \mu_N \sqrt{I(I+1)}, \quad (1)$$

where g_N is the nuclear g factor (5.5856 for a proton) and $\mu_N = eh/(4\pi m_p)$ is the nuclear magneton. Substitution of the charge e and mass of a proton, m_p , gives the value of 5.051×10^{-27} J/T for μ_N . The symbol μ_N is the unit of nuclear magnetic moment and is smaller than the electronic Bohr magneton (μ_B) by the electron-to-proton mass ratio (~ 1800).

The nuclear moment will interact with a local *magnetic induction* (flux density)², B_{loc} , to cause an energy change (the Zeeman effect)

$$E_{\text{Zeeman}} = -g_N \mu_N M_I B_{\text{loc}}. \quad (2)$$

Here, M_I is the quantum number measuring the component of nuclear spin angular momentum (and magnetic moment) along the field direction, which can have values of $-I, -I+1, \dots, +I$. The effect of the field is thus to break the $2I+1$ degeneracy and to produce energy levels whose spacing increases linearly with B_{loc} (or B), as shown in fig. 1. Transitions among these levels can be produced by electromagnetic radiation, provided that the selection rule $\Delta M_I = \pm 1$ is satisfied. In this case, the resonant frequency is given by

$$\nu = \frac{\Delta E_{\text{Zeeman}}}{h} = \frac{g_N \mu_N}{h} B_{\text{loc}}. \quad (3)$$

For protons, $\nu = 4.26 \times 10^7 \cdot B_{\text{loc}}$, where ν is expressed in hertz and B_{loc} is expressed in tesla. For typical fields of 1 T to 20 T, ν falls in the radio-frequency region (10 MHz to 1000 MHz). In practice, values of B_0 (the external applied field) are chosen to fix ν to some convenient value (e.g., 60 MHz, 100 MHz, and 200 MHz).

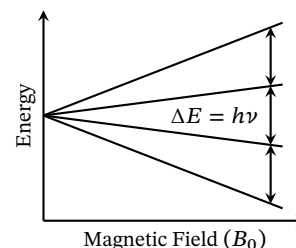


Figure 1: Energy levels and allowed transitions of a nucleus with $I = 3/2$ in a magnetic induction of magnitude B .

² The vector quantity \mathbf{B} is called either the *magnetic induction* or the *magnetic flux density*, although the term *magnetic field strength* is more commonly used. Unfortunately, the name *magnetic field strength* was given to \mathbf{H} at a time when \mathbf{H} was considered to be the fundamental magnetic-field vector. It is now known that \mathbf{B} is the fundamental vector (analogous to \mathbf{E} , the electric-field vector). To add to the confusion, $\mathbf{B} = \mathbf{H}$ in a vacuum when CGS units are used. In the internationally-recognized SI system, $\mathbf{B} = \mu_0 \mathbf{H}$ in a vacuum, and the vacuum permeability $\mu_0 = 4 \times 10^{-7}$ H/m. In SI units, \mathbf{B} is expressed in tesla ($1 \text{ T} = 1 \text{ Wb/m}^2 = 1 \times 10^4 \text{ G}$) and \mathbf{H} is expressed in A/m. In many texts, \mathbf{B} is loosely called the *magnetic field*.

Chemical Shifts

Equation (2) gives the energy levels of a nucleus in the presence of an external applied field. The term B_{loc} is the magnetic induction (*local field*) at the nucleus.

In general, the local induction, B_{loc} , at the nucleus will differ from the externally applied induction, B_0 , because of the magnetization, M , that is induced by B_0 :

$$B_{\text{loc}} = B_0 + \mu_0 M = (1 + \chi) B, \quad (4)$$

where μ_0 is the vacuum permeability and χ is the (dimensionless) volume susceptibility, the magnetic analog of dielectric polarizability.

As most organic compounds are diamagnetic, only the diamagnetic contribution to the susceptibility is important in determining the resonance condition for a given nucleus. The diamagnetic contribution arises because the orbital motion of the electrons is altered by the presence of B_0 so that there is a net orbiting of electrons about the field lines. This circulating charge in turn generates a magnetic induction, B_d , which is proportional and directly opposed to the external field, B_0 . Thus, B_{loc} equals $B_0 + B_d$, with

$$B_d = \chi B_0 = -\sigma B_0, \quad (5)$$

where σ is a positive constant called the *shielding constant*. The resonant frequency of nucleus i becomes

$$\nu_i = \frac{g_N \mu_N}{h} B_{i,\text{loc}} = \frac{g_N \mu_N}{h} B_0 (1 - \sigma). \quad (6)$$

The diamagnetic shielding constant, σ , is generally quite small ($\sim 10^{-5}$) and increases as the electron density around the nucleus is increased. Changes in the local induction ($B_{\text{loc}} = B_0 (1 - \sigma)$), and thus changes in ν , of a few parts per million (ppm) are typical when the chemical environment about a nucleus is changed. The chemical shift in ppm of a nucleus i relative to a reference nucleus r is defined by

$$\delta_i \equiv \frac{\nu_i - \nu_{\text{ref}}}{\nu_{\text{ref}}} \times 10^6 = \frac{\sigma_{\text{ref}} - \sigma_i}{1 - \sigma_{\text{ref}}} \times 10^6 \simeq (\sigma_{\text{ref}} - \sigma_i) \times 10^6. \quad (7)$$

Here, the definition is based on the resonant frequencies for a fixed external induction (field), B_0 .

Tetramethylsilane (TMS) is usually used as the proton reference, since it is chemically inert and its 12 equivalent protons give a single transition at a frequency ν_{ref} , lower than the frequency ν_i found in most organic compounds. Thus, δ is generally positive and increases when substituents are added that attract electrons and thereby reduce the shielding about the proton. This shielding arises because the electrons near the proton are induced to circulate by the applied field B_0 , shown in fig. 2. This electron current produces a secondary field that *opposes* the external field and thus reduces the local field at the nucleus. As a result, resonance at a fixed

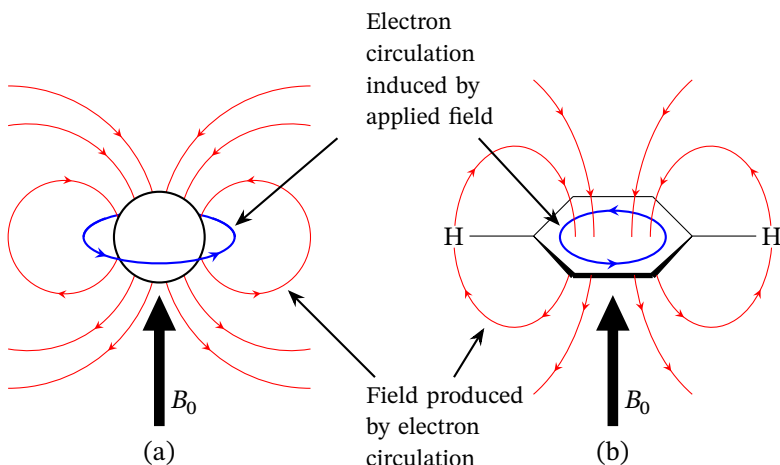


Figure 2: Shielding and deshielding of protons: (a) shielding of a proton due to induced diamagnetic electron circulation; (b) deshielding of protons in benzene due to aromatic ring currents.

field, such as 9.4 T, requires a higher frequency for protons with greater shielding. This shielding effect is generally restricted to electrons localized on the nucleus of interest, since random tumbling of molecules causes the effect of secondary fields due to electrons associated with neighboring nuclei to average to zero. Nuclei such as ^{19}F , ^{13}C , and ^{11}B have more local electrons than hydrogen, hence their chemical shift ranges are much larger.

CH ₃ protons		Acetylenic protons	
(CH ₃) ₄ Si	0.0	HOCH ₂ C≡CH	2.33
(CH ₃) ₄ C	0.92	ClCH ₂ C≡CH	2.40
CH ₃ CH ₂ OH	1.17	CH ₂ COC≡CH	3.17
CH ₃ COCH ₃	2.07	Olefinic protons	
CH ₃ OH	3.38	(CH ₃) ₂ C=CH ₂	4.6
CH ₃ F	4.30	Cyclohexene	5.57
CH ₂ protons		CH ₂ CH=CHCHO	6.05
Cyclopropane	0.22	Cl ₂ C=CHCl	6.45
CH ₃ (CH ₂) ₄ CH ₃	1.25	Aromatic protons	
(CH ₃ CH ₂) ₂ CO	2.39	Benzene	7.27
CH ₃ COCH ₂ COOCH ₃	3.48	C ₆ H ₅ CN	7.54
CH ₃ CH ₂ OH	3.59	Naphthalene	7.73
CH protons		α-Pyridine	8.50
Bicyclo[2.2.1]heptane	2.19	Aldehydic protons	
Chlorocyclopropane	2.95	CH ₃ OCHO	8.03
(CH ₃) ₂ CHOH	3.95	CH ₃ CHO	9.72
(CH ₃) ₂ CHBr	4.17	C ₆ H ₅ CHO	9.96

Table 1: Typical proton chemical shifts δ (ppm).

Long-range *deshielding* can occur in aromatic and other molecules with delocalized π electrons. For example, when the plane of the benzene molecule is oriented perpendicular to B_0 , circulation of the π electrons

produces a ring current, illustrated in fig. 2. This ring current induces a secondary field at the protons that is aligned *parallel* to B_0 and results in a higher local field for the protons. This induced field changes with benzen orientation, but does not average to zero, since it is not spherically symmetric. Because of this net deshielding effect, the resonance of the benzene protons occurs at a relatively low external field. The proton chemical shift δ for benzene is 7.27 ppm, much higher in frequency from the value $\delta = 1.43$ ppm that is observed for cyclohexane, in which ring currents do not occur. Similar deshielding values of δ for different functional groups are shown in table 1, and additional values are available in refs. [3–7]. Although the resonances change somewhat for different compounds, the range for a given functional group is usually small and δ values are widely used for structural characterization in organic chemistry.

Spin-Spin Splitting

High-resolution NMR spectra of most organic compounds reveal more complicated spectra than those predicted by eq. (6), with transitions often appearing as multiplets. Such *spin-spin splitting patterns* arise because the magnetic moments of one nucleus (A) can interact with that of a nearby nucleus (B), causing a small energy shift up or down depending on the relative orientations of the two moments. The energy levels of nucleus A then have the form

$$E_A = -g_{N_A}\mu_N M_{I_A} (1 - \sigma_A) B_0 + hJ_{AB} M_{I_A} M_{I_B} \quad (8)$$

and there is a similar expression for E_B . The spin-spin interaction is characterized by the coupling constant J_{AB} , and the effect is to split the energy levels in the manner illustrated for acetaldehyde in fig. 3. It is apparent from this diagram that the external field B_0 does not affect the small spin-spin splitting that is characterized by the coupling constant J . The quantity J is a measure of the strength of the pairwise interaction of the spin nucleus A with the spin of nucleus B. Since there are only proton-proton interactions in acetaldehyde, the same splitting occurs for both CH and CH₃ resonances.

The total integrated intensity of the CH and CH₃ multiplets follows the proton ratio of 1 : 3. However, the intensity distribution within each multiplet is determined by the relative population of the lower level in each transition. Since the level spacing is much less than kT , the Boltzmann population factors are essentially identical for these levels. However, there is some degeneracy because rapid rotation of the CH₃ group around the C–C bond makes the three protons magnetically equivalent. The number of spin orientations of the CH₃ protons that produced equivalent fields at the CH proton determine the degeneracy. The eight permutations of the CH₃ spins shown in fig. 3 thus lead to

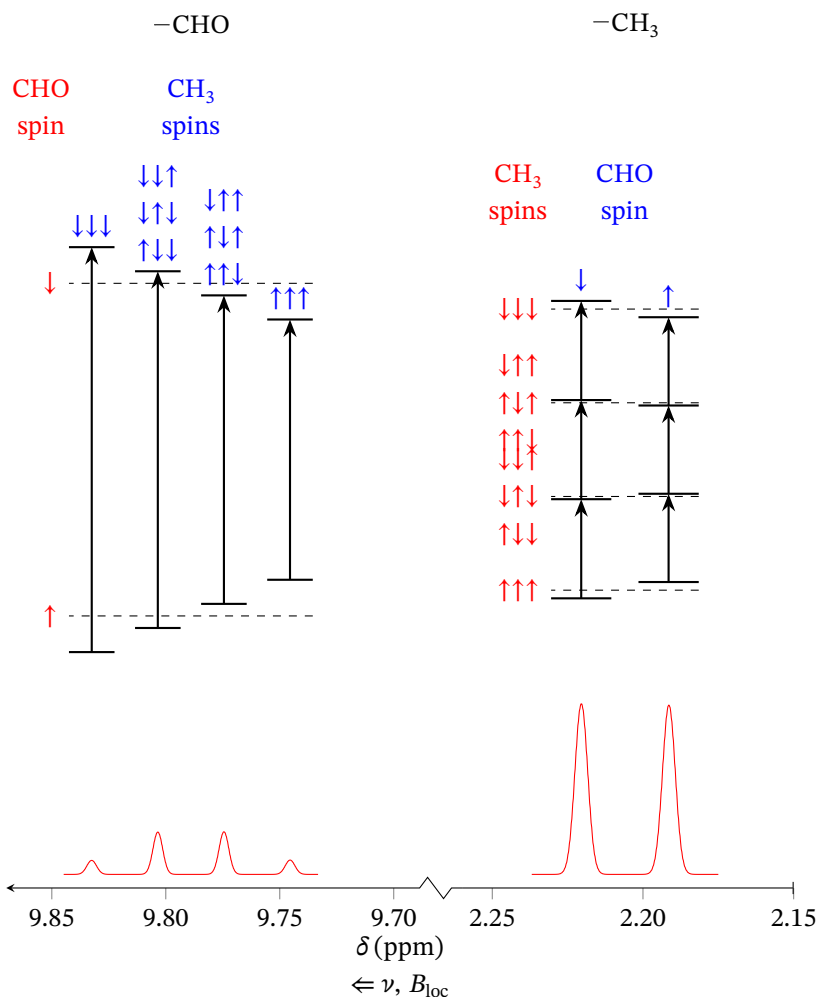


Figure 3: Energy levels, transitions, and the NMR spectrum for acetaldehyde (CH_3CHO) at 100 MHz. The coupling constant for the system is $J = J_{\text{CH}_3} = J_{\text{CHO}} = 2.09 \text{ Hz}$. For CHO, the quantum number $M_I = \pm \frac{1}{2}$. For the CH_3 group, $M_I = \pm \frac{1}{2}, \pm \frac{3}{2}$. The dashed lines represent the level spacing that would occur in the absence of the spin-spin interaction. The spacing of the energy levels are greatly exaggerated in the figure.

a predicted intensity ratio of 1:3:3:1 for the CH multiplet. Similarly, the CH_3 doublet peaks will be of equal intensity, with a total integrated intensity three times that of the CH peaks. In a more general sense, it can be seen that n equivalent protons interacting with a different proton will split its resonance into $n + 1$ lines whose relative intensities are given by coefficients of the terms in the binomial expansion of the expression $(\alpha + \beta)^n$. Equivalent protons also interact and produce splittings in the energy levels. However, these splittings are symmetric for upper and lower energy states, so no new NMR resonances are produced.

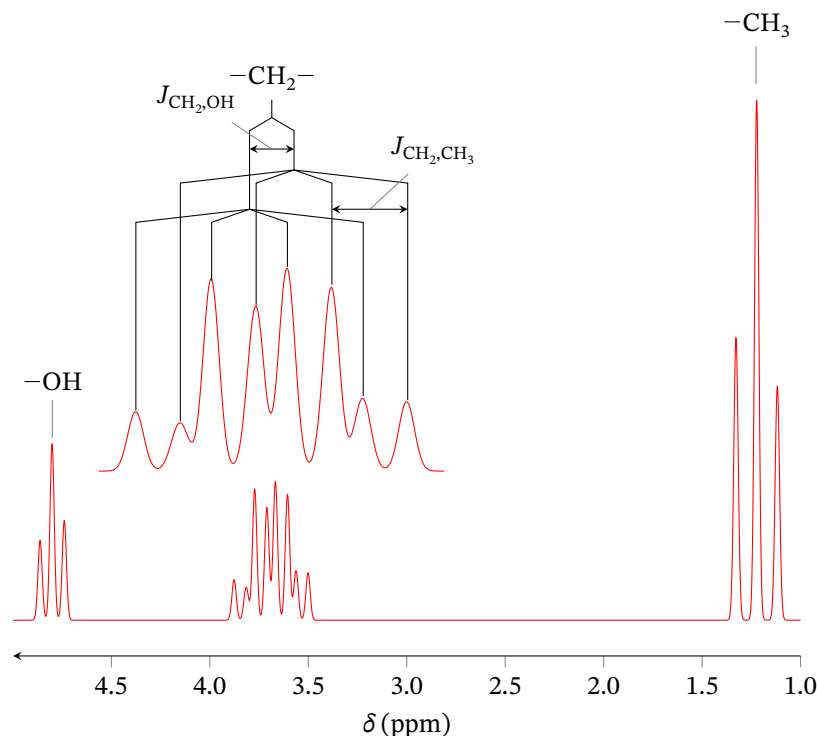


Figure 4: Simulated NMR spectrum of highly purified ethanol at 90 MHz.

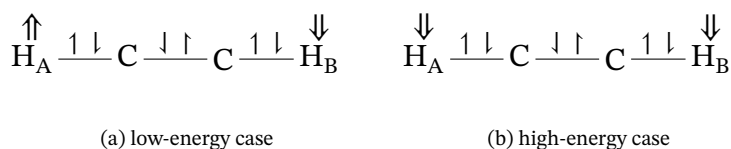
If a proton is coupled to more than one type of neighboring nucleus, the resultant multiplet pattern can often be understood as a simple stepwise coupling involving different J values. For example, the CH_2 octet that occurs for pure $\text{CH}_3\text{CH}_2\text{OH}$ shown in fig. 4 arises from OH doublet splitting ($J = 4.80$ Hz) of the quartet of lines caused by coupling ($J = 7.15$ Hz) with CH_3 . It should be mentioned that such regular splitting and intensity patterns are expected for two nuclei A and B only if $|\nu_A - \nu_B| \gtrsim 10 J_{AB}$. The spectra for this weakly coupled case are termed *first order*. Since the difference $\nu_A - \nu_B$ (in Hz) increases with field while J_{AB} does not, NMR spectra obtained with a high-field instrument (600 MHz) are often easier to interpret than those from a low-field spectrometer (>200 MHz). However, even if the multiplets are not well separated, it is still possible to deduced accurate chemical shifts and J values using slightly more involved procedures, which are outlined in most texts on NMR spectroscopy.[5–9] Such an exercise can be done as an optional part of this experiment, although it will not be necessary for the determination of equilibrium constants.

The mechanism of spin–spin coupling is known to be indirect and to involve the electrons in the bonds between interacting nuclei. The spin of nucleus A is preferentially coupled antiparallel to the nearest bonding electron through the *Fermi contact interaction*, which is significant only when the electron density is nonzero at the first nucleus.³ This

Coupling	(Hz)
	–20 to 5
	2 to 9
	0
	0 to 3.5
	6 to 14
	11 to 19
	ortho- 6 to 9 meta- 1 to 3 para- 1

Table 2: Typical proton spin–spin coupling constants

³ Such is the case only for electrons in s orbitals, since p , d , and f orbital wavefunctions have nodes at the nucleus.



electron-spin alignment information is transmitted by electron-electron interactions to nucleus B to produce a field that thus depends on the spin orientation of the first nucleus, illustrated in fig. 5. Since the strength of this interaction falls off rapidly with separation, only neighboring groups produce significant splitting. A few typical spin-spin coupling constants are given in table 2. These, along with the chemical shifts, served to identify proton functional groups. As mentioned above, the multiplet intensities also give useful information about neighboring groups. Thus NMR spectra can provide detailed structural information about large and complex biomolecules.

Rotational Energy Barrier

In *N,N*-dimethylacetamide, the two *N*-methyl groups can undergo chemical exchange through a process analogous to a *cis-trans* isomerization, where the product is chemically identical to the reactant. Due to the

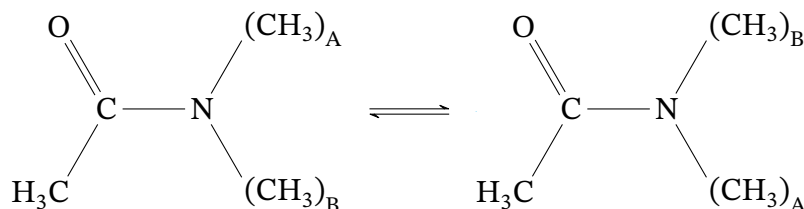


Figure 6: Isomerization of dimethylacetamide

characteristic period of the NMR measurement, a large range of reaction rates relevant in the chemical laboratory is easily accessible (10^{-1} to 10^{-5}). In addition, rotational barriers in the range of 3 kcal/mol to 20 kcal/mol can be studied by this method.^[10]

Arrhenius and Eyring equations

The Arrhenius equation (eq. (9)) describes the temperature dependence of reaction rates. It provides a simple, empirical method for finding the activation energy for a process by observing the change in reaction rate as a function of temperature.

$$k = A \exp \left\{ \frac{-E_a}{RT} \right\} \quad (9)$$

As stated earlier, k is the rate constant of the reaction. T is the absolute temperature (in K), A is a pre-exponential factor, constant and specific to each reaction, E_a is the activation energy for the process (with the same units as RT), and R is the universal gas constant. By taking the

Figure 5: Illustration of nuclear spin-spin interaction transmitted via polarization of bonding electrons. The two electrons about each carbon will tend to be parallel, since this arrangement minimizes the electron-electron repulsion (Hund's rule for electrons in degenerate orbitals).

natural logarithm of each side and rearranging a bit, the equation can be transformed into the following:

$$\ln k = \frac{-E_a}{R} \frac{1}{T} + \ln A. \quad (10)$$

This version makes $\ln k$ a linear function of T^{-1} with a slope of $-E_a/R$, resulting in a much easier task of curve-fitting.

An extension of the Arrhenius equation, the Eyring equation (eq. (11)), is used in Transition State Theory to describe the enthalpy (ΔH^\ddagger), entropy (ΔS^\ddagger), and Gibbs free energy (ΔG^\ddagger) of the transition state.

$$k = \kappa \frac{k_B T}{h} \exp\left\{\frac{\Delta G^\ddagger}{RT}\right\} \quad (11)$$

Recall that k_B and h are Boltzmann's constant and Planck's constant, respectively. The constant κ represents the *transmission coefficient* and accounts for the possibility that a complex might cross back through a transition state without becoming a product. The transmission coefficient is generally assumed to be 1. If we recall that ΔG^\ddagger can be expressed as $\Delta G^\ddagger = \Delta H^\ddagger + T\Delta S^\ddagger$, eq. (11) becomes

$$k = \kappa \frac{k_B T}{h} \exp\left\{\frac{\Delta S^\ddagger}{R}\right\} \exp\left\{-\frac{\Delta H^\ddagger}{RT}\right\}. \quad (12)$$

Again, if we take the natural logarithm of eq. (12), we obtain

$$\ln \frac{k}{T} = \frac{-\Delta H^\ddagger}{R} \frac{1}{T} + \ln \frac{\kappa B}{h} + \frac{\Delta S^\ddagger}{R}. \quad (13)$$

With this form, we can fit a straight line to the reaction rate data as a function of $1/T$ and solve for ΔG^\ddagger , ΔH^\ddagger , and ΔS^\ddagger .

Line Shape Analysis

If two groups of chemically equivalent nuclei are exchanged by an intramolecular process, the NMR spectrum is a function of the difference in their resonance frequencies, $\nu_A - \nu_B = \Delta\nu$, and of the rate of exchange, k .⁴ The effects of exchange at several temperatures on the linewidths at ν_A and ν_B are shown in ???. At low temperatures, the exchange is slow and $k \ll \Delta\nu$. The spectrum thus consists of two sharp singlets at ν_A and ν_B (???). At high temperatures, the exchange is fast (i.e., $k \gg \Delta\nu$) and a single sharp peak is observed (???). There is also an intermediate temperature range over which the spectrum consists of two significantly broadened overlapping lines (???).

Usually, spin-spin and spin-lattice relaxation determine the width of an NMR absorption peak.[11] Here, we are concerned with the additional effect of exchange of two groups of chemically equivalent nuclei on linewidth. The Heisenberg uncertainty principle states that the product of the uncertainty in the measurement of the energy of a particular state, ΔE ,

⁴ A typical value for $\Delta\nu$ is about 10 Hz.

and the uncertainty in the lifetime of the state, Δt , is approximately equal to the reduced Planck's constant, $\hbar = h/(2\pi)$:

$$\Delta E \Delta t \simeq \hbar. \quad (14)$$

Since

$$\Delta E = h\Delta\nu_{1/2}, \quad (15)$$

where $\Delta\nu_{1/2}$, the absorption linewidth for the transition, is inversely proportional to the lifetime of the excited state:

$$\Delta\nu_{1/2} = \frac{\Delta E}{h} = \frac{\Delta E \Delta t}{h \Delta t} = \frac{1}{2\pi \Delta t}. \quad (16)$$

An exact analysis of the line broadening produced by the exchange process is derived from the Bloch equations.^[10] The Bloch equations describe the motion of the bulk magnetic moment of a sample in the presence of a static field, B_0 , and a rotating field, B_1 , perpendicular to B_0 .

The exact function for the lineshape^[12] in the case of two equivalent exchanging groups with no coupling is given by

$$g(\nu) = \frac{K\tau(\nu_A - \nu_B)^2}{\left[\frac{1}{2}(\nu_A - \nu_B) - \nu\right]^2 + [2\pi\tau(\nu_A - \nu)(\nu_B - \nu)]^2}, \quad (17)$$

where $g(\nu)$ is the intensity at the frequency, ν , K is a normalization constant, and $\tau = 1/(2k)$, where k is the rate constant for the exchange. The variables τ , ν_A , and ν_B are functions of temperature and cannot be determined separately. Values for these three may be estimated with a fitting algorithm⁵ to generate a curve-of-best fit for $g(\nu)$. Alternatively, various approximations can be made which apply over different ranges of exchange rates.

⁵ Such as the [Scipy optimization library](#).

Approximate Methods for Evaluation of Rate Constants^[13]

Direct calculation of the lifetime of a specific spin state from eq. (17) can be made over a limited temperature range. Beyond a certain temperature, the rate of exchange is so fast that the magnetic environments of the two sets of nuclei are identical and any possible distinction between the two sets of nuclei is lost. Thus we have only one set of spins with a lifetime determined by the spin-spin and spin-lattice relaxation mechanisms.

As the temperature is varied from values at which the rate of exchange is low through values of intermediate exchange rates, to rapid exchange, a series of approximations is available for the calculation of lifetimes. although these approximate methods provide somewhat less accurate results than does eq. (17), they present the student with a meaningful treatment of the data obtained by an NMR study of a chemical rate process.

Slow and Intermediate Exchange

At slow exchange rates, the spectrum consists of two lines. In this region, $\tau \gg (\nu_A)^{-1}$, and eq. (17) reduces to

$$g(\nu)_A = g(\nu)_B = \frac{KT'_{2A}}{1 + [T'_{2A}(\nu_A - \nu)]^2}, \quad (18)$$

where T'_{2A} is the spin-spin relaxation time. Comparison of ?? to the exact function shows that the linewidth of the line at ν_A is

$$(\Delta\nu_A)_{1/2} = \frac{1}{\pi} \left(\frac{1}{T'_{2A}} + \frac{1}{\tau_A} \right). \quad (19)$$

In the absence of exchange, the linewidth is $(\Delta\nu_0)_{1/2} = (\pi T'_{2A})^{-1}$. Exchange results in *broadening* equal to $(\pi\tau_A)^{-1}$. A value for $k (= 1/(2\tau))$ is determined by comparing linewidths at half height of exchanging peaks to those of peaks recorded at temperatures where the rate of exchange is very small:

$$k = \pi [(\Delta\nu_e)_{1/2} - (\Delta\nu_0)_{1/2}]. \quad (20)$$

For slow exchange, the rate can also be related to the change in *peak separation*. Equation (21) applies over the limited range where there is extensive overlap between the two separate peaks, but where they have not yet coalesced (see below):

$$k = \frac{\pi}{\sqrt{2}} \sqrt{\Delta\nu_0^2 - \Delta\nu_e^2}, \quad (21)$$

where $\Delta\nu_i$ is the peak separation in Hz, and the subscripts ($i = e$ or 0) have the previously defined meanings.⁶

A third method applies in the slow exchange region. In the *ratio method*, k is calculated from the ratio of the intensities of the peaks, I_{\max} , to the intensity midway between the peaks, I_{\min} , $r = I_{\max}/I_{\min}$ and

$$k = \frac{\pi\Delta\nu_0}{\sqrt{2}} (r + \sqrt{r^2 - 1})^{-1/2}. \quad (22)$$

Coalescence Temperature

The coalescence temperature is defined as the temperature at which the appearance of the spectrum changes from that of two separate peaks to that of a single, flat-topped peak (see ??). At this temperature, building on eq. (22),

$$k = \frac{\pi\Delta\nu_0}{\sqrt{2}}. \quad (23)$$

Fast Exchange

At temperatures above the coalescence temperature, the spectrum consists of a single peak. In this region, $\tau \ll (\nu_A - \nu_B)^{-1}$ and eq. (17) reduces to

$$g(\nu) = \frac{KT'_2}{1 + \pi T'_2(\nu_A + \nu_B - 2\nu)^2}. \quad (24)$$

⁶ In other words, $\Delta\nu_e$ should range from $\Delta\nu_0$ at very low temperatures to 0 at high temperatures.

If the signal is not completely collapsed, i.e., the process is slow enough to contribute to its width but is still well beyond the rate corresponding to separate signals, the following approximation results:

$$k = \frac{\pi \Delta \nu_0^2}{2} [(\Delta \nu_e)_{1/2} - (\Delta \nu_0)_{1/2}]^{-1} \quad (25)$$

Safety Precautions

Dimethyl sulfoxide (DMSO, $(\text{CH}_3)_2\text{SO}$) is relatively non-toxic, but can rapidly carry other compounds through the skin. Gloves should be worn whenever handling it. *N,N*-dimethylacetamide (DMA, $\text{CH}_3\text{C}(\text{O})\text{N}(\text{CH}_3)_2$) is toxic and students should avoid inhalation and skin contact. Carry out all solution preparations in a fume hood or well-ventilated area. Dispose of waste chemicals as instructed.

Procedure

1. Prepare a 15 vol% solution of DMA and DMSO- d_6 in a 1.5 mL to 2.0 mL microfuge tube. Use a 1000 μL micropipettor to add an appropriate amount ($\sim 600 \mu\text{L}$) of the solution to a clean NMR tube.
2. Record ^1H -NMR spectra for the solution at 10 K increments from 293 K to 403 K.
3. Peak widths, positions, and intensities should be measured using the TopSpin software on the NMR lab computers and this data should be exported with the spectra for later analysis.

Data Analysis

1. Correctly assign all peaks in the spectrum using table 1 and other NMR reference sources.[5–9] Mark solvent peaks with an asterisk (*). If splitting patterns deviate from your expectations, discuss possible reasons for the deviation.
2. The data extracted from TopSpin should be split into three groups corresponding to slow/intermediate exchange, coalescence temperature, and fast exchange.
3. Using eq. (20) through eq. (25), to calculate values for k at each temperature.
4. Create a plot of $\ln k$ as a function of $1/T$. The slope of this plot yields a value for ΔG^\ddagger . Compare this value to literature values for this rotational barrier.
5. Values for ΔH^\ddagger and ΔS^\ddagger can be calculated from the value obtained for ΔG^\ddagger in the previous step. Error propagation formulae for these values have been published in Morse et al. [14].

Questions and Further Thoughts

1. Briefly discuss your assignments of chemical shifts and spin–spin splitting patterns of *N,N*-dimethylacetamide.
2. Compare your values of ΔG^\ddagger with those for the gas phase (see values in Jarek, Flesher, and Shin [15]). What solvent properties might account for any differences you observe?

Lab Report Guidelines

Your lab report should consist of the following parts:

Title, Author and Date

Experimental Procedure This should be a very brief general outline of the procedure, written out as a paragraph or two. Give the make and model for any major instruments you used, as well as any important settings. For fluorescence spectroscopy, this especially means the excitation wavelength and slit widths.

Results and Discussion This should include an overview of the analyzed data and responses to the questions worked into a natural narrative.

References

Appendix At the very end of your report, include examples of any calculations that you did by hand. Provide digital copies of the Excel (or other) files that you used to generate your graphs.

You do *not* need to include uncertainty calculations for this lab.

References

- [1] Francis P. Gasparro and Nancy H. Kolodny. “NMR determination of the rotational barrier in *N,N*-dimethylacetamide. A physical chemistry experiment”. In: *Journal of Chemical Education* 54.4 (1977), p. 258. DOI: [10.1021/ed054p258](https://doi.org/10.1021/ed054p258).
- [2] JW Nibler et al. *Experiments in Physical Chemistry*. 9th ed. McGraw-Hill, New York, 2014.
- [3] C Pouchert and J Behnke. *The Aldrich Library of ^{13}C and ^1H FT-NMR Spectra*. Vol. 1–3. Aldrich Chemical Co., 1993.
- [4] National Institute of Advanced Industrial Science and Technology. *SDBSWeb*. URL: <https://sdb.s.db.aist.go.jp> (visited on 02/21/2020).

- [5] RM Silverstein et al. *Spectrometric Identification of Organic Compounds*. 8th ed. Wiley-Interscience, New York, 2014.
- [6] John Anthony Pople, William George Schneider, and Harold Joseph Bernstein. *High-Resolution Nuclear Magnetic Resonance*. McGraw-Hill, New York, 1959.
- [7] Jefferson C Davis Jr. *Advanced Physical Chemistry: Molecules, Structure, And Spectra*. Wiley-Interscience, New York, 1965.
- [8] Max T. Rogers and Jane L. Burdett. “Keto–Enol Tautomerism In β -Dicarbonyls Studied By Nuclear Magnetic Resonance Spectroscopy: Ii. Solvent Effects On Proton Chemical Shifts And On Equilibrium Constants”. In: *Canadian Journal of Chemistry* 43.5 (1965), pp. 1516–1526. DOI: [10.1139/v65-202](https://doi.org/10.1139/v65-202).
- [9] Jane L. Burdett and Max T. Rogers. “Keto-Enol Tautomerism in β -Dicarbonyls Studied by Nuclear Magnetic Resonance Spectroscopy.1 I. Proton Chemical Shifts and Equilibrium Constants of Pure Compounds”. In: *Journal of the American Chemical Society* 86.11 (1964), pp. 2105–2109. DOI: [10.1021/ja01065a003](https://doi.org/10.1021/ja01065a003).
- [10] FA Bovey. “Nuclear Magnetic Resonance Spectroscopy”. In: Academic Press, New York, 1969. Chap. VII.
- [11] Malcolm H Levitt. “Spin Dynamics: Basics of Nuclear Magnetic Resonance”. In: John Wiley & Sons, 2008. Chap. 12.
- [12] Alan Carrington and Andrew D McLachlan. “Introduction to Magnetic Resonance”. In: New York: Harper and Row, 1967, pp. 205–208.
- [13] ES Johnson. “Advances in Magnetic Resonance”. In: ed. by JS Waugh. Vol. 1. New York: Academic Press, 1965. Chap. 2, pp. 64–68.
- [14] Paige M. Morse et al. “A Static Agostic α -CH \cdots CH \cdots M Interaction Observable by NMR Spectroscopy: Synthesis of the Chromium(II) Alkyl [Cr₂(CH₂SiMe₃)₆]₂- and Its Conversion to the Unusual ”Windowpane” Bis(metallacycle) Complex [Cr(κ -2-C,C’-CH₂SiMe₂CH₂)₂]₂-. In: *Organometallics* 13.5 (1994), pp. 1646–1655. DOI: [10.1021/om00017a023](https://doi.org/10.1021/om00017a023).
- [15] Russell L. Jarek, Robert J. Flesher, and Seung Koo Shin. “Kinetics of Internal Rotation of N,N-Dimethylacetamide: A Spin-Saturation Transfer Experiment”. In: *Journal of Chemical Education* 74.8 (1997), p. 978. DOI: [10.1021/ed074p978](https://doi.org/10.1021/ed074p978).

Further Reading

- Kevin F. Morris and Luther E. Erickson. “NMR Determination of Internal Rotation Rates and Rotational Energy Barriers: A Physical

- Chemistry Lab Project”. In: *Journal of Chemical Education* 73.5 (May 1, 1996), p. 471. DOI: [10.1021/ed073p471](https://doi.org/10.1021/ed073p471).
- Michael M. Folkendt et al. “Gas-phase proton NMR studies of keto-enol tautomerism of acetylacetone, methyl acetoacetate, and ethyl acetoacetate”. In: *The Journal of Physical Chemistry* 89.15 (1985), pp. 3347–3352. DOI: [10.1021/j100261a038](https://doi.org/10.1021/j100261a038).
 - Jeremy KM Sanders and Brian K Hunter. *Modern NMR Spectroscopy: A Guide For Chemists*. 2nd ed. Oxford University Press, New York, 1993.
 - Robin Kingsley Harris. *Nuclear Magnetic Resonance Spectroscopy*. John Wiley & Sons Inc., New York, 1986.
 - Russell S Drago. “Physical Methods For Chemists”. In: 2nd ed. Saunders, Philadelphia, 1992. Chap. 7, 8.
 - RJ Abraham, J Fischer, and P Loftus. *Introduction to NMR spectroscopy*. Wiley-Interscience, New York, 1990.
 - Charles P Slichter. *Principles Of Magnetic Resonance*. 3rd ed. Springer International Publishing, 1990.